Oncogenic role of RNA-binding protein GNL2 in glioma: Promotion of tumor development through enhancing protein synthesis

XUDONG YANG and XIANGDONG LI

Department of Neurosurgery, The First Affiliated Hospital, Soochow University, Suzhou, Jiangsu 215008, P.R. China

Received July 19, 2023; Accepted February 27, 2024

DOI: 10.3892/ol.2024.14440

Abstract. RNA-binding proteins (RBPs) are aberrantly expressed in various diseases, including glioma. In the present study, the role and mechanism of RBPs in glioma were investigated. Differentially expressed genes (DEGs) in glioma were screened from public databases and overlapping genes between DEGs and RBPs were selected in a bioinformatics analysis to identify the hub gene. Next, evaluation of expression, survival analysis and cell experiments were performed to examine the impact of the hub gene on glioma. Through bioinformatics analysis, G protein nucleolar 2 (GNL2), programmed cell death 11 (PDCD11) and ribosomal protein S6 (RPS6) were identified as potential biomarkers in glioma prognosis and GNL2 was chosen as the hub gene for further investigation. GNL2 was increased in glioma tissues and related to poor survival outcomes. Cell experiments revealed that GNL2 knockdown inhibited glioma cell growth, migration and invasion. In addition, GNL2 was found to affect the overall protein synthesis of ribosomal protein L11 in glioma cells. In conclusion, GNL2, PDCD11 and RPS6 may serve as potential biomarkers in glioma prognosis. Importantly, GNL2 acts as an oncogene in glioma and it enhances protein synthesis to promote the development of brain glioma.

Introduction

Glioma, a primary central nervous system tumor, comprises 45.2% of all intracranial neoplasms, with an annual incidence between 0.003 and 0.005% (1). Gliomas range in grade from I to IV: Higher-grade gliomas (III and IV) are characterized by aggressive, poorly differentiated cells, while low-grade gliomas (LGG, I and II) consist of slowly proliferating, well-differentiated cells (2). The cornerstone of glioma management involves a multimodal approach encompassing chemotherapy, surgical resection and radiation therapy (3,4). Although surgical assistance and molecular pathology have developed rapidly in recent times, the efficacy in patients with glioma remains poor due to its high recurrence rate, short survival time, aggressive growth and strong invasiveness (5,6). Thus, the continued exploration of glioma mechanisms is critical to identifying prospective clinical indicators.

RNA-binding proteins (RBPs), ubiquitously present in all living organisms, were first discovered in yeast and mammalian cell extracts due to their ability to interact with RNA molecules (7). In human embryonic kidney cells, more than a thousand proteins have been identified to be able to bind with RNAs. These proteins participate in numerous biological functions beyond dictating the fate of RNA molecules (8). A study by Muleya and Marondedze (9) suggested that unallocated RBP may have a key role in adjusting metabolic changes in response to multiple stressful stimuli. Furthermore, the life-cycle of RNA transcription and processing from the nucleus to translation and degradation in the cytoplasm is influenced by several related proteins, including numerous RBPs (10). In all kinds of organisms, from yeast to humans, cap structures are co-transcriptionally affixed to the 5' end of RNA. When coupled with polymerase II transcripts, this cap structure becomes an essential signal for binding these transcripts to downstream proteins (11). Despite these insights, further investigation is necessary to clarify the mechanisms of RBPs in human disease pathology.

The present study delved into the role and mechanisms of RBPs in gliomas to identify key RBPs with clinical value and to explore the potential impact of the central gene G protein nucleolar 2 (GNL2) on glioma progression. It was hypothesized that aberrant expression of RBPs is a driver of glioma progression and the identification of key RBPs among them (e.g., GNL2) may render them potential prognostic biomarkers. As a pivotal gene, GNL2 has a crucial role in the pathogenesis of gliomas by influencing key cellular processes, particularly enhanced protein synthesis, which ultimately contributes to the development of gliomas. These findings provide insight into targeted therapies for gliomas based on

Correspondence to: Dr Xiangdong Li, Department of Neurosurgery, The First Affiliated Hospital, Soochow University, 188 Shizi Street, Gusu, Suzhou, Jiangsu 215008, P.R. China
E-mail: xdlijia@aliyun.com

Key words: glioma, RNA-binding protein, GNL2, prognosis, protein synthesis

regulatory RNA-binding proteins and lay the foundation for future identification of new biomarkers and development of therapeutic strategies. The present study provides important scientific support to deepen the understanding of the molecular mechanisms of gliomas and develop more individualized therapeutic options for patients.

Materials and methods

Identification of differentially expressed RBPs in glioma samples. The identification analysis from the The Cancer Genome Atlas (TCGA) dataset was conducted using R software (version 3.3.1; https://www.r-project.org/) and the edgeR package. The criteria for identifying differentially expressed genes (DEGs) were set as follows: Fold change (FC) <0.5 for downregulated genes and FC >2 for upregulated genes, and P<0.05 for each. The heatmap and volcano map were plotted by the gplots package of R software. A list of genes encoding RBPs was referenced from the reference 'a census of human RNA-binding proteins' (12). The overlapping genes between the RBP-encoding genes and the identified DEGs were determined by the Venn package of R software.

Functional enrichment and prognostic analysis of key overlapping genes. Interactions between proteins are crucial for exploring tumor mechanisms. In the present study, protein-protein interaction (PPI) analyses of the overlapping genes were built using the Search Tool for the Retrieval of Interacting Genes and proteins (STRING; https://string-db.org). Next, 'Molecular Complex Detection' (MCODE) function in Cytoscape software (version 3.7.2; https://cytoscape.org), a clustering algorithm based on a node-weighted algorithm, was used to identify highly interacting gene clusters. Next, Gene Ontology (GO) analysis was performed on the genes screened by MCODE based on the Database for Annotation, Visualization and Integrated Discovery (DAVID; https://david.ncifcrf.gov/) database. Subsequently, overlapping genes were analyzed for overall survival (OS) prognosis by univariate Cox regression, and hazard ratios (HR), P-values and confidence intervals (CI) for hazard coefficients were shown in a forest plot.

Construction of prognostic risk model. A prognostic gene signature was constructed using the least absolute shrinkage and selection operator (LASSO) regression method, implemented through the 'glmnet' package in R software, to predict glioma prognosis. Ten-fold cross-validation was used to extract the ideal value from the least partial likelihood deviation in order to increase objectivity and dependability. The average risk score was applied to classify patients into high-risk and low-risk groups. Kaplan-Meier (KM) survival curves were generated using the 'survival' package in R software to evaluate OS probabilities in two groups, with the log-rank test used to determine statistical significance. A receiver operating characteristic (ROC) curve was drawn to assess the prediction accuracy of the risk model. To gauge how well the model predicted patient survival, the area under the curve (AUC) value was calculated.

Predictive nomogram construction with key genes related to glioma prognosis. Next, a univariate/multivariate Cox regression analysis was performed on the top 10 prognosis-related genes using the 'survival' package of R software, and forest plots were generated with the 'forest plot' package of R software to display the variables available as nomograms. A total of 3 key genes were selected due to their high association with glioma prognosis. The 'rms' program (https://CRAN.R-project.org/package=rms) in R software was then employed to create a nomogram to forecast the 1-, 3- and 5-year OS rates. The closeness of the Nomogram model to the calibration curve resembles the model's prediction ability.

Expression level and survival analyses on the hub gene. Based on the above analysis, one hub gene (GNL2) was selected in the present study for the next analysis. First, the levels of GNL2 in LGG and glioblastoma (GBM) samples were compared using GEPIA (http://gepia.cancer-pku.cn). Following this, the association between GNL2 levels and various survival probabilities, including disease-specific survival (DSS), OS and progression-free survival (PFS), was systematically investigated utilizing the KM plotter online database (https://kmplot.com). The log-rank P-values and HRs were calculated with 95% CIs to measure the statistical significance of the observed differences in survival outcomes.

Cell culture and transfection. Glioma cell lines (U251MG, SW1783 and U373) and normal human astrocyte cells (NHA) were obtained from the Chinese Academy of Sciences Cell Bank (Shanghai, China). They were kept in DMEM with 10% FBS (Absin) at 37˚C with 5% CO_2. For transfection, cells were seeded in appropriate culture vessels and transfected with siRNAs targeting GNL2 (si-GNL2 #1, si-GNL2 #2 and si-GNL2 #3) or control small interfering RNA (siRNA) following the manufacturer's instructions for Lipofectamine 3000 reagent (Invitrogen; Thermo Fisher Scientific, Inc.). The relevant sequence information was as follows: si-GNL2#1, 5'-CACGTGTGATTAAGCAGTCATCATT-3'; si-GNL2#2, 5'-CCATACAAAGTTGTCATGAAGCAAA-3'; si-GNL2#3, 5'-GGGGTTCTCCACTTTAGGTTAA-3'; and si-negative control (si-NC), 5'-UUCUCCGAACGUGUCACGUTT-3'.

Western blot (WB) analysis. Cells were lysed in RIPA buffer with a protease inhibitor cocktail (Sigma-Aldrich; Merck KGaA) on ice for 30 min. To obtain nuclear and cytosolic extracts, the cell lysates were centrifuged at 800 x g for 5 min at 4˚C to pellet the nuclei. The supernatant with the cytosolic fraction was transferred to a fresh tube, and the nuclear pellet was resuspended in a nuclear extraction buffer. After centrifuging lysates at 14,000 x g for 15 min at 4˚C, the supernatant was collected. Protein concentrations were determined using the BCA protein assay kit from Thermo Fisher Scientific, Inc. 10% SDS-PAGE was used to separate identical quantities of protein (30-50 g) before they were transferred to PVDF membranes (EMD Millipore). The membranes were first treated with 5% non-fat milk in Tris-buffered saline containing Tween-20 (TBST) for 1 h at room temperature (~25˚C) to block them. Following this, the membranes were incubated overnight with primary antibodies at 4˚C at the following dilutions: Anti-GNL2 (1:1,000 dilution; Abcam),

anti-Lamin A/C (1:1,000 dilution; Cell Signaling Technology, Inc.), anti-ribosomal protein L11 (RPL11; 1:1,000 dilution; Abcam) and anti-Tubulin (1:2,000 dilution; Cell Signaling Technology, Inc.). TBST was used to wash the membranes and then horseradish peroxidase-conjugated secondary antibody (1:2,000 dilution; Cell Signaling Technology, Inc.) was applied for 1 h at room temperature. Enhanced chemiluminescence substrate (Beyotime Institute of Biotechnology) was employed to detect signals and a chemiluminescence imaging system (Bio-Rad ChemiDoc; Bio-Rad Laboratories, Inc.) was used for visualization. Finally, protein bands were quantified using ImageJ software (version 1.51; National Institutes of Health).

Reverse transcription-quantitative PCR (RT-qPCR). Total RNA was extracted from the cells using TRIzol reagent (Invitrogen; Thermo Fisher Scientific, Inc.). A NanoDrop 2000 spectrophotometer (Thermo Fisher Scientific, Inc.) was employed to determine the purity and concentration of the RNA. cDNA was generated from 1 g of total RNA by using a High-capacity cDNA RT kit (Applied Biosystems; Thermo Fisher Scientific, Inc.) according to the manufacturer's instructions. qPCR was performed on an Applied Biosystems 7500 Fast real-time PCR machine (Thermo Fisher Scientific, Inc.) using SYBR Green Master Mix (Sangon Biotech Co., Ltd.) according to the manufacturer's instructions. For the qPCR, the thermocycling conditions were as follows: 10 min of initial denaturation at 95˚C and 40 cycles of denaturation at 95˚C for 15 sec and 1 min of annealing and extension at 60˚C. The primer sequences used were as follows: GNL2 forward, 5'-ATCCAAATGTTGGCAAGAGC-3' and reverse, 5'-ACACCTGGACAGTCAATCAGG-3'; GAPDH forward, 5'-TGCACCACCAACTGCTTAGC-3' and reverse, 5'-GGCATGGACTGTGGTCATGAG-3'. The relative gene expression was calculated using the $2^{-\Delta\Delta Cq}$ method (13), with GAPDH as the internal control.

Cell Counting Kit-8 (CCK-8) assay. The impact of si-GNL2 #2 on SW1783 and U373 cells was determined using a CCK-8 (Beyotime Institute of Biotechnology). Cellular samples were seeded in 96-well plates and subjected to transfection with si-GNL2 #2 or control siRNA. Following transfection, the cells were incubated for 0, 1, 2, 3 or 4 days. To evaluate cell proliferation, 10 μl of CCK-8 solution was added to each well and allowed to incubate at 37˚C for 2 h. Subsequently, a microplate reader was used to measure the optical density values at 450 nm.

Transwell assay. The impact of si-GNL2 #2 on the invasion and migration of SW1783 and U373 cells was assessed using Transwell assays. For the invasion assay, the upper chamber of a 24-well Transwell plate (8 μm pore size; Nanjing KeyGen Biotech Co., Ltd.) was coated with Matrigel® (Beijing Solarbio Science & Technology Co., Ltd.). Following transfection with either si-GNL2 #2 or control siRNA, the cells were suspended in serum-free medium and then seeded in the upper chamber. Simultaneously, medium supplemented with 10% FBS was added to the lower chamber. After 24 h of incubation at 37˚C, the non-migrated cells on the upper surface of the membrane were gently removed with a cotton swab. Cells that migrated to the lower surface were then fixed with 4% paraformaldehyde for 20 min at room temperature and stained with DAPI for 15 min. After staining, cells were washed, dried and counted under a light microscope. The migration assay was performed in a similar manner to the invasion assay, with the key difference being the omission of Matrigel® in the Transwell plate to allow for the assessment of cell migration without extracellular matrix components.

Labeling and detection of newly synthesized proteins. Based on a previous study (14), 100 μCi of ^{35}S-methionine/^{35}S-cysteine (EXPRE^{35}S^{35}S Protein Labeling Mix; Perkin Elmer) was added to each ml of cell culture half an hour before the end of cell treatment to label newly generated proteins. Following treatment, cells were lysed in a modified RIPA solution containing protease and phosphatase inhibitors (Beijing Solarbio Science & Technology Co., Ltd.) after being rinsed with PBS. Using a Bradford Protein Assay Kit (Bio-Rad Laboratories, Inc.), the protein concentrations were measured, and 50 μg of the extract was placed on Whatman paper following the protocol described in Tailler *et al* (14). Using a cold 5% trichloroacetic acid (TCA) and methionine solution, polypeptides were precipitated. This was followed by boiling in 5% TCA for 15 min and washing with ethanol. Subsequently, 30 μg of radiolabeled proteins were separated by 10% SDS-PAGE, transferred to a PVDF membrane and scintillation was measured with a Typhoon FLA 7000 machine (GE Healthcare).

Statistical analysis. All experimental results were expressed as the mean ± standard deviation from a minimum of three separate experiments. Student's t-test was used to compare differences between two groups. One-way ANOVA was performed for comparisons between multiple groups, followed by Tukey's post-hoc test to adjust for multiple comparisons. $P<0.05$ was considered to indicate a statistically significant difference. All statistical analyses were conducted using the SPSS 25.0 software package (IBM Corp.). Graphs were generated using GraphPad Prism 8.0 (GraphPad Software; Dotmatics).

Results

Identification of 1,063 overlapping genes from TCGA-DEGs and RBPs. The volcano plot (Fig. 1A) revealed 8,739 upregulated and 426 downregulated DEGs related to glioma in the TCGA dataset. The Venn package was applied to analyze the intersecting genes between up- and down-regulated DEGs and genes encoding RBPs, respectively. As presented in Fig. 1B, the overlapping genes included 1,037 upregulated and 26 downregulated genes. These overlapping genes were specifically selected for further investigation in the present study, as they may shed light on the molecular mechanisms underlying glioma and potentially represent valuable therapeutic targets.

PPI network construction and module analysis. To further explore the relationship between glioma and the intersecting genes, a PPI network was generated to reveal the interaction between these genes. The genes were imported into Cytoscape and analyzed using the plugin MCODE, resulting in a PPI network with 194 nodes and 11,364 edges (Fig. 1C). GO term

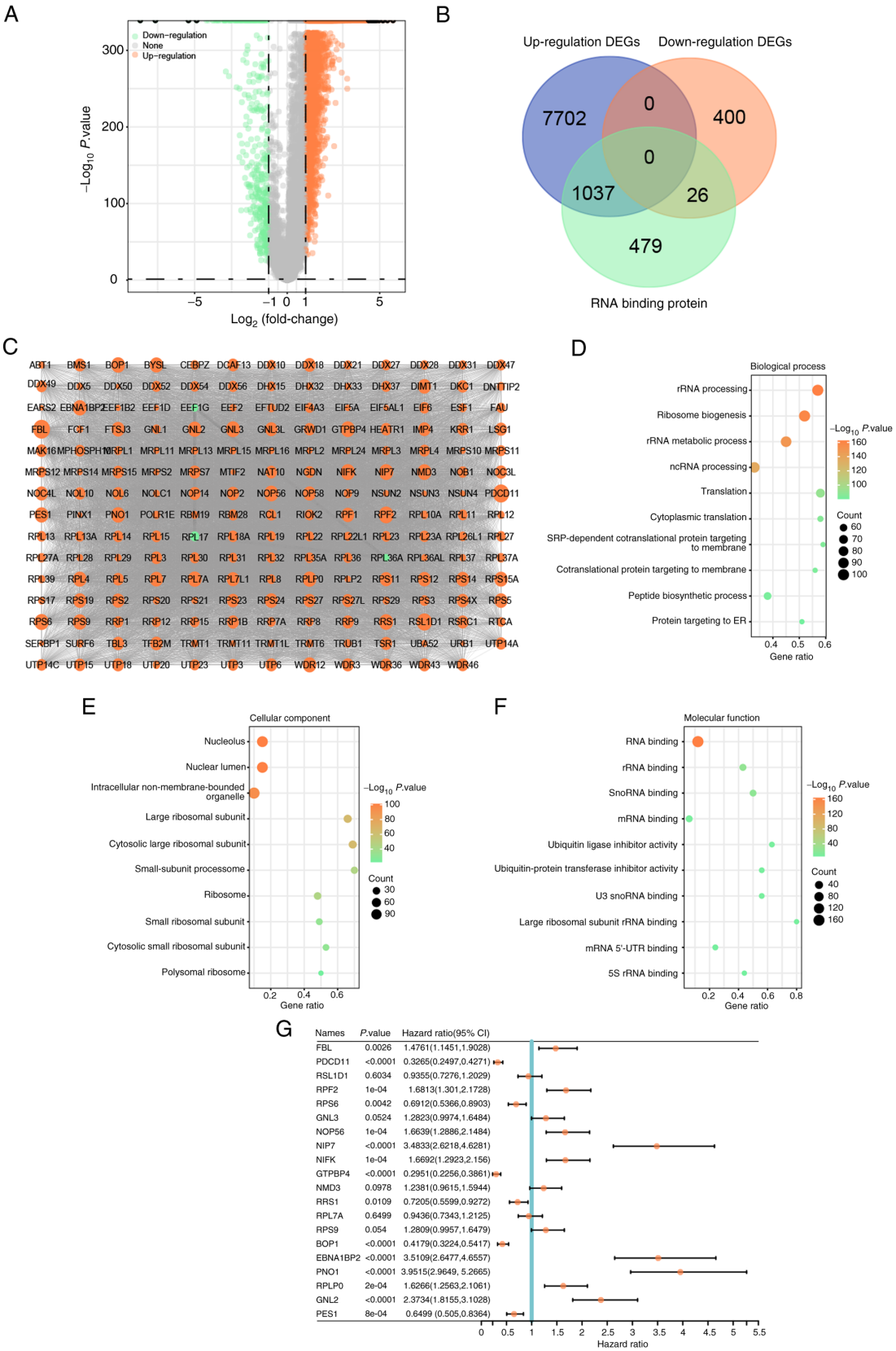

Figure 1. Intersection analysis of DEGs and RBP-encoding genes. (A) Volcano plot displays the distribution of DEGs, with upregulated DEGs in orange and down-regulated DEGs in green. The threshold for significance is indicated by the horizontal line. (B) Venn diagram of the overlapping genes between DEGs and genes encoding RBPs (1,037 up- and 26 downregulated DEGs). (C) Identification of highly interconnected gene modules using MCODE analysis. Nodes represent genes and edges represent interactions between genes. Orange nodes represent upregulated DEGs and green nodes represent downregulated DEGs. The size of the nodes reflects the degree of connectivity within the module. (D-F) Bubble plot representation of Gene Ontology term enrichment analyses. (D) Biological process, (E) cellular component and (F) molecular function. The size of the bubbles indicates the number of DEGs associated with each term or pathway, while the color represents the adjusted P-value, with orange representing higher significance and green representing lower significance. (G) Forest plot showing the results of univariate Cox analysis of the top 20 genes. Each horizontal line represents a gene and the length represents the 95% CI of the hazard ratio. DEG, differentially expressed gene; RBP, RNA-binding protein.

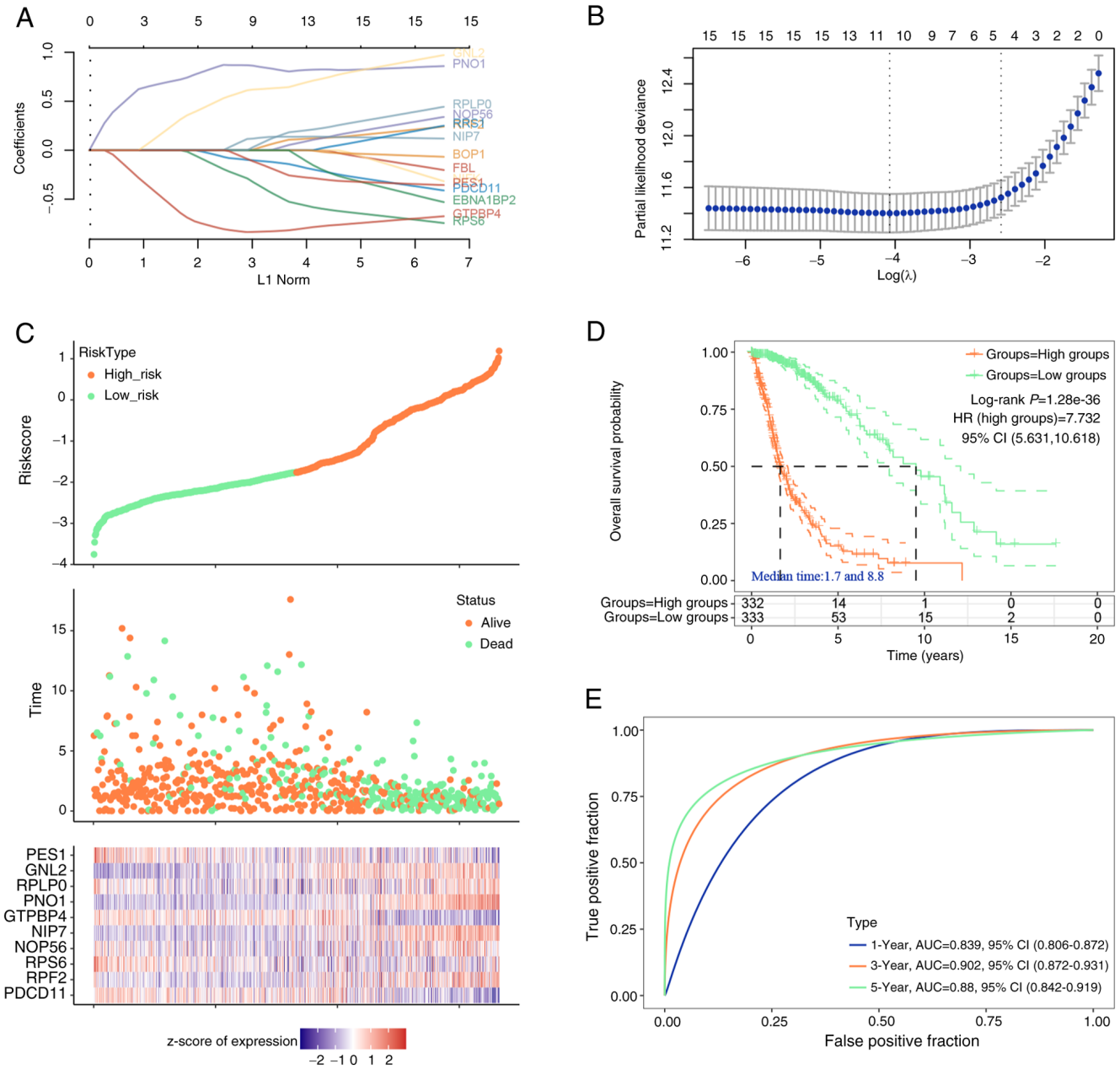

Figure 2. Risk prognostic analysis of the top 20 signature genes. (A) Lasso proportional hazards regression displaying the coefficient profiles of the top 20 significant genes. (B) Selection of the optimal gene signature using 10-fold cross-validation, resulting in the identification of 10 candidate genes. (C) Risk model analysis. The top panel shows the risk score distribution of glioma patients, the middle panel shows the survival status and time of patients in the low-risk and high-risk groups and the bottom panel shows the heat map of the expression profiles of 10 prognostic genes in the low-risk and high-risk groups. (D) Kaplan-Meier survival curve analysis comparing overall survival between high-risk (n=332) and low-risk (n=333) groups. (E) ROC curve analysis of the risk model at 1, 3 and 5 years. A larger AUC value indicates a higher predictive ability of the model. HR, hazard ratio; AUC, area under the ROC curve; ROC, receiver operating characteristic.

enrichment analysis was then performed on 194 genes. In the GO enrichment results, the main enrichment items of these genes in cellular component, biological process and molecular function included 'ribosomal RNA (rRNA) processing', 'ribosome biogenesis', 'large ribosomal subunit', 'RNA binding' and 'large ribosomal subunit rRNA binding' (Fig. 1D-F). After performing OS prognostic analysis on 194 genes, the results of the top 20 signature genes ($P<0.05$) were selected for visualization in a forest plot (Fig. 1G). These 20 genes may be used as prognostic genes for glioma and progressed to the subsequent analysis.

Prognostic risk model of the top 20 genes. The top 20 significant genes were used for Lasso proportional hazards regression and 10-fold cross-validation to construct the optimal gene signature, and 10 candidate genes were finally determined (Fig. 2A and B). The risk scores, survival duration and status of the glioma patients, along with a heatmap detailing z-score normalized expression of prognostic genes derived from the TCGA-glioma dataset, were illustrated in Fig. 2C. Each column in the heat map represents a gene expression profile for an individual patient and corresponds to the patient data shown in the risk and survival plots above. To identify RBP features

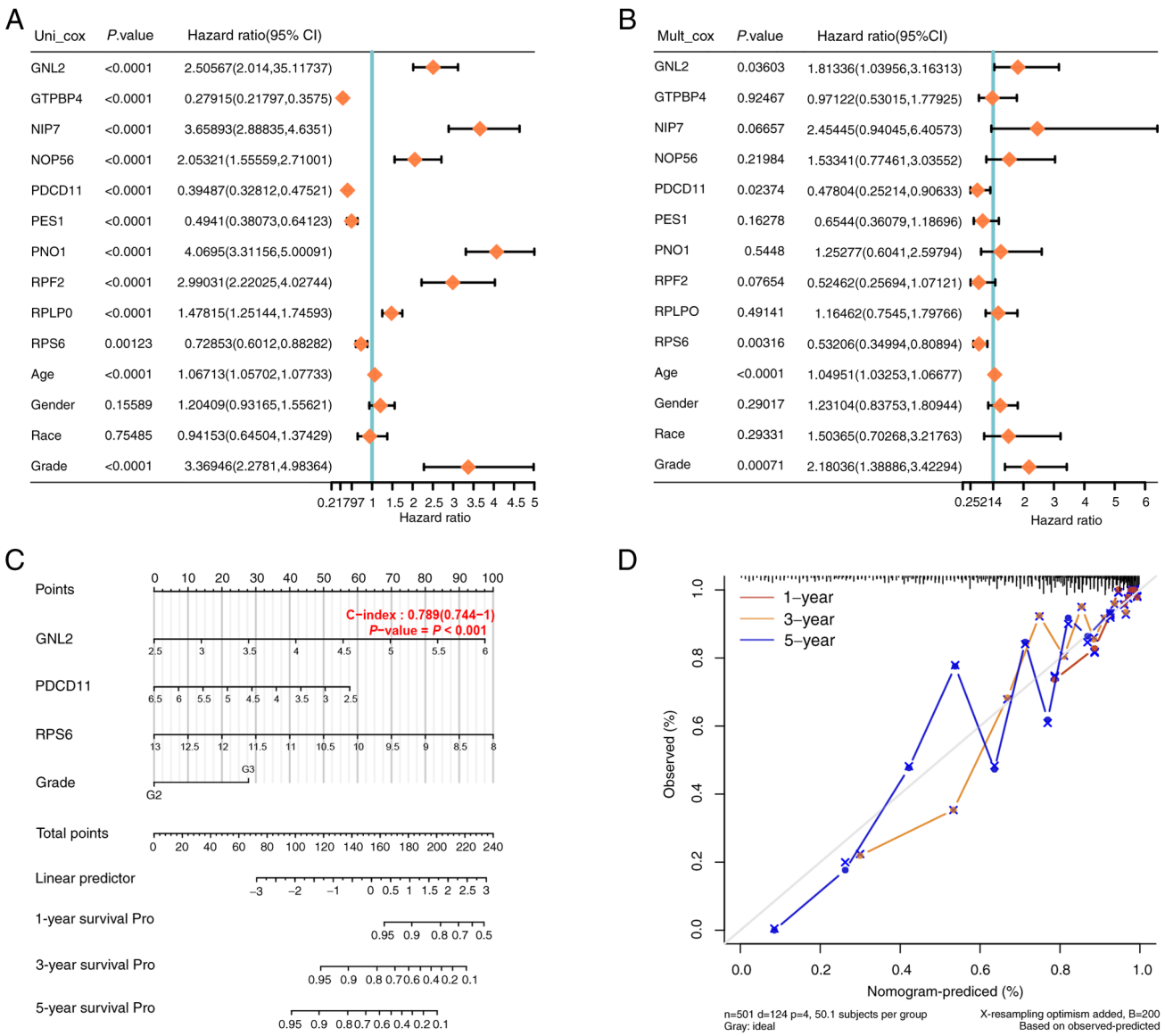

Figure 3. Prognostic analysis and Nomogram construction for patients with glioma. (A) Univariate and (B) multivariate Cox regression analysis of 10 genes and clinical variables; forest plots showing P-value, hazard ratio and 95% CI for each prognostic factor. (C) Nomogram integrating GNL2, PDCD11, RPS6 and Grade to predict 1-, 3- and 5-year overall survival time in patients with glioma. (D) Calibration plots of nomograms for the consistency check between 1-, 3- and 5-year OS predictions and actual outcomes. GNL2, G protein nucleolar 2; PDCD11, programmed cell death 11; RPS6, ribosomal protein S6; Pro, probability.

suitable for survival prediction, patients with glioma, based on the average risk score, were classified into low-risk (n=333) and high-risk groups (n=332). KM curve analysis indicated that compared to low-risk patients, high-risk individuals had worse OS (Fig. 2D). Furthermore, ROC curves demonstrated that the AUC of the risk model at 1, 3 and 5 years was 0.839, 0.902 and 0.88 in the training set, respectively (Fig. 2E), which indicated the good predictive ability of this model.

Construction and verification of the nomogram of glioma prognosis. Univariate/multivariate Cox regression analyses were performed on the 10 genes and clinical variables included in the prognostic risk model. GNL2, programmed cell death 11 (PDCD11), ribosomal protein S6 (RPS6) and Grade (P<0.05) were suggested to be independent prognostic indicators for OS (Fig. 3A and B). To establish a more reliable clinical prediction method, a comprehensive nomogram containing GNL2, PDCD11, RPS6 and Grade was constructed to predict 1-, 3- and 5-year OS for patients with glioma (Fig. 3C). The calibration plot of patient survival prediction in the TCGA-glioma cohort showed that the predicted results of the prognostic nomogram were similar to the actual results (Fig. 3D). The GNL2, PDCD11 and RPS6 genes may serve as new biomarkers in glioma prognosis. In the present study, GNL2 was chosen to be the target gene for further analysis.

Expression and prognostic analysis of GNL2 in glioma. Next, the levels of GNL2 were analyzed in LGG and GBM, and it was found that the levels of GNL2 in LGG and GBM were higher than those in normal tissues (Fig. 4A). In the OS, PFS and DSS analyses, the survival rate of patients with high GNL2 expression was lower (Fig. 4B-D). Collectively, these findings indicate that GNL2 functions as an oncogene in glioma.

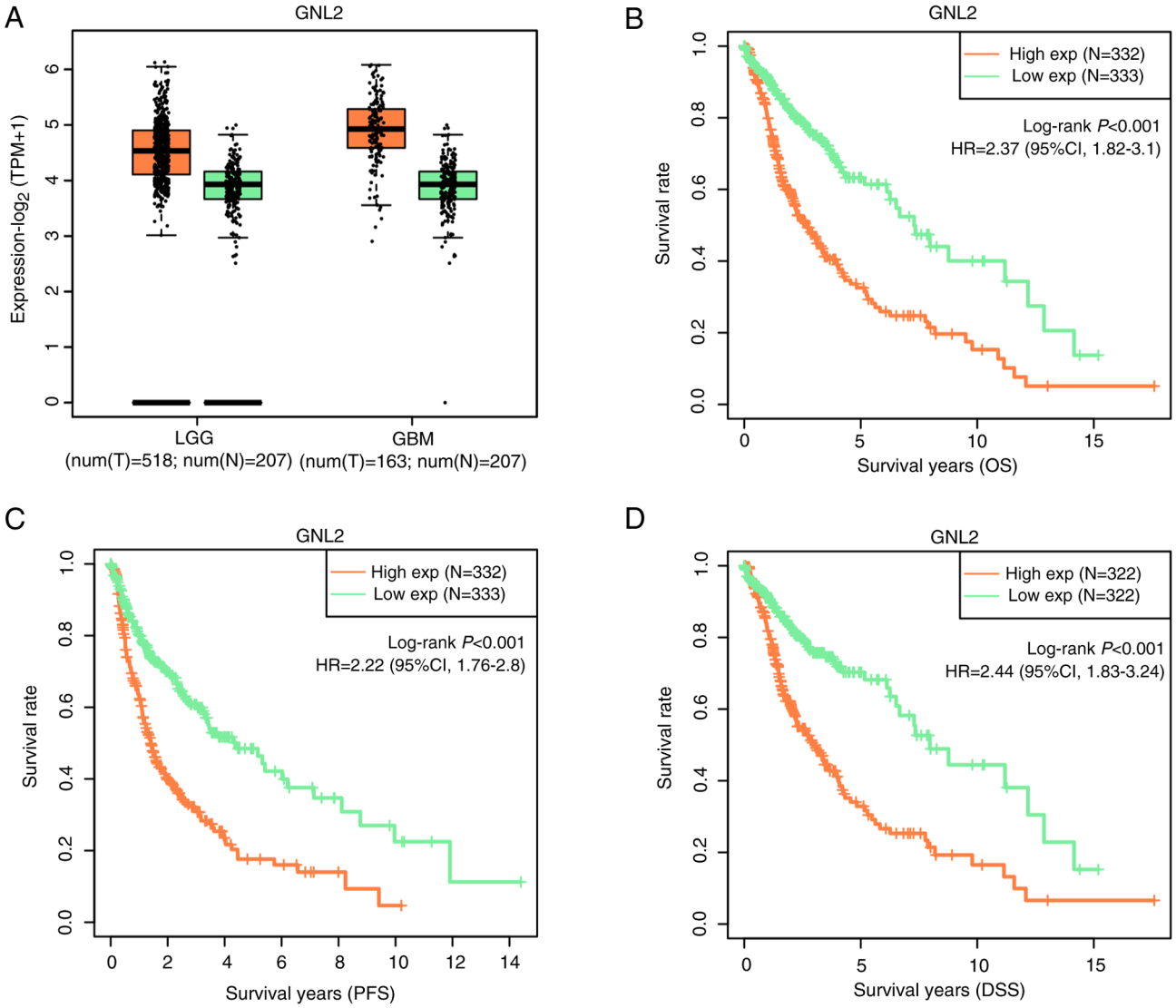

Figure 4. GNL2 expression and its association with survival in patients with glioma. (A) GEPIA database detects the expression level of GNL2 in LGG and GBM; the orange box line represents tumor samples and the green box line represents normal samples. Each box plot shows the median expression level (central line), the 25 to 75th percentiles (box) and the standard error of the mean (Whisker lines). (B-D) KM survival curve analysis of the effect of GNL2 expression on (B) OS, (C) PFS and (D) DSS in patients with glioma. The horizontal axis displays the survival time, while the vertical axis shows the survival probability. GNL2, G protein nucleolar 2; LGG, low-grade glioma; GBM, glioblastoma; OS, overall survival; PFS, progression-free survival; DSS, disease-specific survival; exp, expression; T, tumor; N, normal tissue sample; HR, hazard ratio.

Knockdown of GNL2 suppresses the proliferation, invasion and migration of glioma cells. By RT-qPCR and WB analyses, the levels of GNL2 were examined in glioma cells and normal cells. The results demonstrated enhanced levels of GNL2 in glioma cells, with particularly pronounced increases observed in the SW1783 and U373 cell lines (Fig. 5A and B). Subsequently, GNL2 was silenced within glioma cell lines using three distinct siRNAs: si-GNL2 #1, si-GNL2 #2 and si-GNL2 #3. Among these, si-GNL2 #2 demonstrated the most optimal knockdown efficiency, as validated by both WB and RT-qPCR (Fig. 5C-F). After further investigation using CCK-8 and Transwell assays, in GNL2-knockdown glioma cell lines, a significant reduction in cell proliferation, invasion and migration was detected in comparison to the control group (Fig. 6A-D). In summary, the present results suggest that GNL2 is a potential oncogene in glioma and its inhibition may impair key oncogenic characteristics of glioma cells, highlighting its prospective value as a therapeutic target.

GNL2 silencing alters RPL11 localization and suppresses protein synthesis in glioma cells. GNL2 is involved in various processes related to rRNA synthesis and processing, and assembly of ribosomal subunits (15,16). According to earlier research, the cytoplasmic/nuclear ratio of 60S ribosomal protein RPL11 was decreased in ovarian cancer cells when GNL2 was silenced (17). In the present study, the protein lysates from SW1783 and U373 cells transfected with si-GNL2 or si-NC we separated into nuclear and cytoplasmic fractions and the localization of RPL11 was assessed using WB. Following the knockdown of GNL2, the expression of RPL11 increased in the nuclei of both SW1783 and U373 cells (Fig. 7A), suggesting that the export of 60S ribosomal subunits was impaired, and GNL2 knockdown decreased the cytoplasmic/nuclear ratio

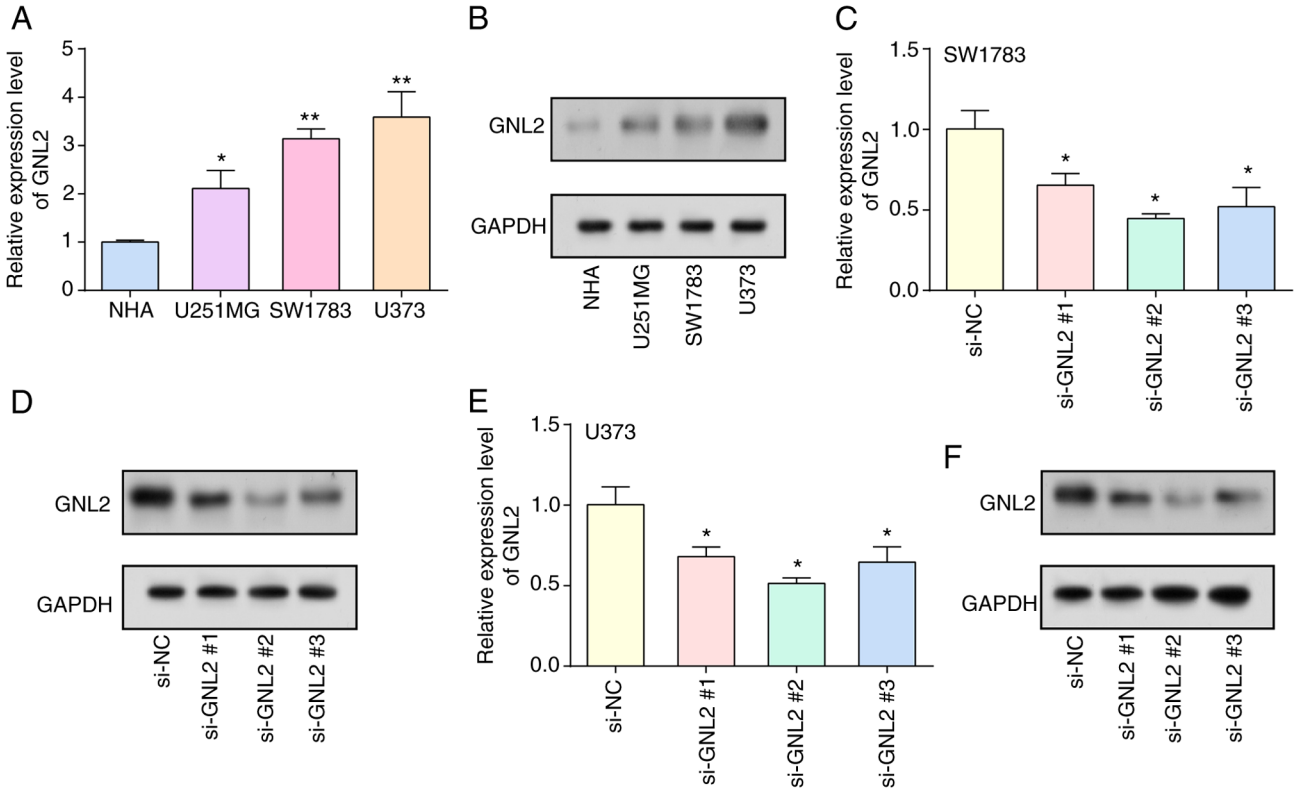

Figure 5. GNL2 protein levels and knockdown efficiency in glioma cell lines. (A and B) Expression levels of GNL2 in glioma cell lines (U521MG, SW1783, U373) and normal control cells (NHA) were determined through (A) RT-qPCR and (B) WB techniques. (C-F) Knockdown efficiency of GNL2 in glioma cells transfected with si-GNL2 #1, si-GNL2 #2 and si-GNL2 #3 was evaluated. (C) RT-qPCR analysis and (D) WB of SW1783 cells and (E) RT-qPCR analysis and (F) WB of U373 cells. *P<0.05, **P<0.01 vs. NHA or NC. GNL2, G protein nucleolar 2; NC, negative control; si, small interfering RNA; RT-qPCR, reverse transcription-quantitative PCR; WB, western blot.

of RPL11. Furthermore, by examining newly synthesized S^{35}-tagged total protein, it was found that knockdown of GNL2 inhibited overall protein synthesis in glioma cells (Fig. 7B). These findings underscore a vital function for GNL2 in the modulation of RPL11 localization and protein synthesis in glioma cells. Silencing of GNL2 appears to disrupt the nuclear export of RPL11, affecting the normal distribution of RPL11 and overall protein synthesis within the cell. These disruptions may potentially influence the oncogenic behavior of glioma cells. The present study thereby suggests that GNL2 may be a potential therapeutic target in glioma.

Discussion

Gliomas account for ~45% of all intracranial tumors (18). The prognosis of patients with glioma patients often deteriorates with increasing degree of malignancy, leading to gliomas being one of the deadliest malignant tumor types, particularly in the context of grade IV GBM (19). Alarmingly, statistics suggest that individuals afflicted with grade IV GBM exhibit a median survival duration of just one year and <5% survive beyond five years (20). Given their malignant nature, surgical intervention or radiation therapy rarely yield curative results for malignant gliomas (21), thereby necessitating the frequent recourse to chemotherapy. However, the effectiveness of chemotherapy is often significantly impeded by the blood-brain barrier, which restricts the entry of intravenously administered anticancer drugs into the glioma region (22). While molecular-targeted therapies have somewhat improved the survival rates of patients with glioma, the overall therapeutic efficacy remains disappointing (23). Given these challenges, it is of utmost importance to further our understanding of the molecular underpinnings of gliomas.

In the current investigation, an exhaustive analysis of glioma samples from the TCGA database was performed, leading to the identification of 8,739 upregulated and 426 downregulated DEGs. To further refine this analysis, the DEGs were cross-referenced with genes encoding RBPs, employing the Venn package, and an intersection of 1,037 up- and 26 downregulated genes was obtained. This set of overlapping genes, potentially crucial in illuminating the molecular underpinnings of glioma, was chosen for subsequent scrutiny in the present study, suggesting their potential as valuable therapeutic targets. To unveil the roles of these crossover genes in glioma, a PPI network comprising 194 genes was constructed. This network not only revealed the interaction of these genes, but also elucidated their potential synergy in glioma pathogenesis. Of note, GO term enrichment analysis for these 194 genes unveiled significant enrichment in functional terms such as 'rRNA processing', 'ribosome biogenesis', 'large ribosomal subunit', 'RNA binding' and 'large ribosomal subunit rRNA binding'. These processes and components are integral for the cellular functioning and protein synthesis machinery (24,25), highlighting the potential relevance of these genes in the context of the aggressive cellular behavior and uncontrolled proliferation of glioma.

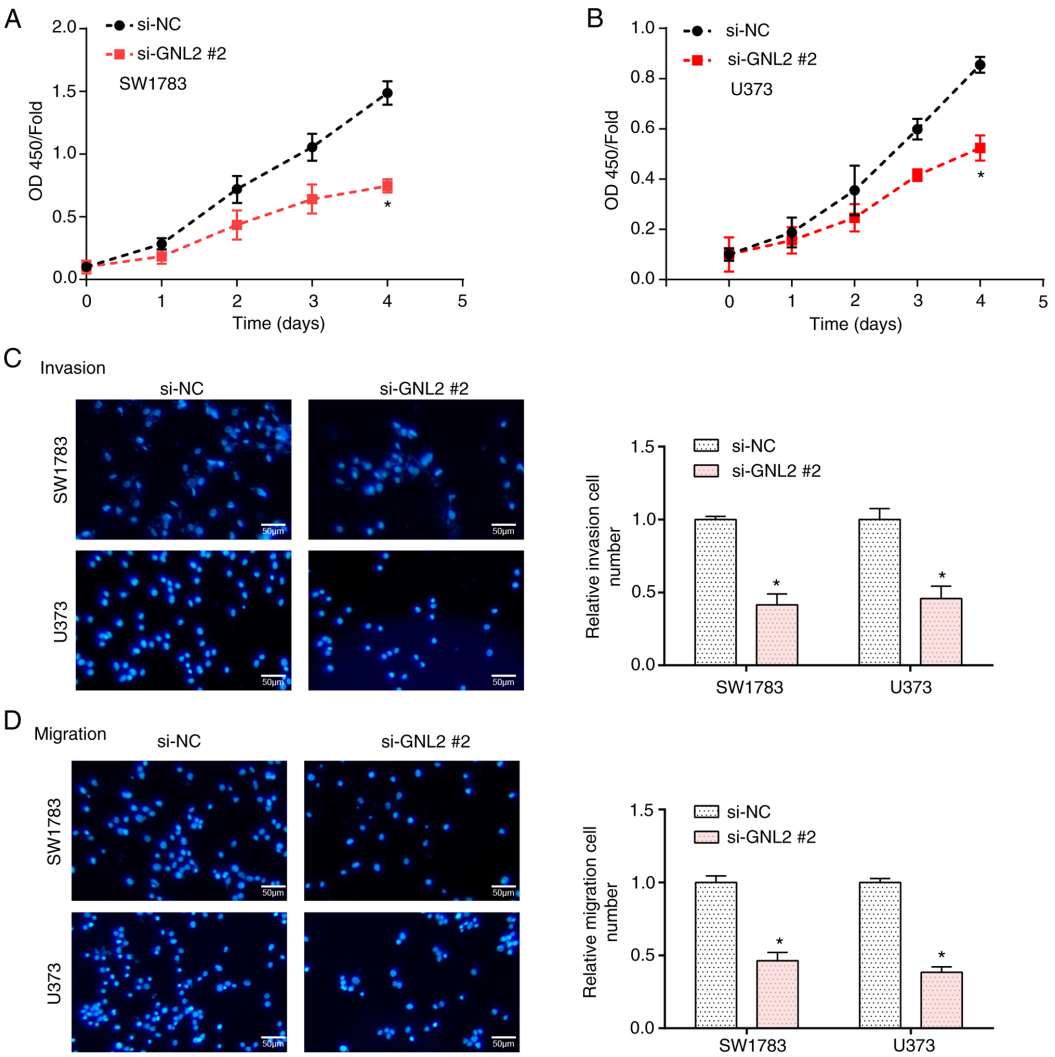

Figure 6. GNL2 knockdown inhibits the proliferation, migration and invasion of glioma cells. (A and B) The effect of GNL2 knockdown on the proliferation of (A) SW1783 and (B) U373 cells was examined by a Cell Counting Kit-8 assay. (C and D) Transwell detection of the effect of GNL2 knockdown on the (C) invasion and (D) migration of SW1783 and U373 cells (scale bar, 50 μm). *P<0.05 vs. NC. GNL2, G protein nucleolar 2; NC, negative control; si, small interfering RNA; OD 450, optical density at 450 nm.

Following an OS prognostic analysis conducted on 194 genes, the top 20 genes with a significant impact on outcomes were selected. These genes were further subjected to LASSO regression, risk model analysis and univariate/multivariate Cox regression analyses to establish a prognostic nomogram for patients with glioma. In the nomogram, 3 genes with clinical value in glioma prognosis were found, namely GNL2, PDCD11 and RPS6. PDCD11, also known as ALG4, NFBP, RRP5 and ALG-4, an NF-κB-binding protein necessary for rRNA maturation and the production of 18S rRNA, colocalizes with U3 RNA in the nucleolus (26,27). To date, only a small number of studies on PDCD11 have been published. Xing *et al* (28) analyzed predictive biomarkers for triple-negative breast cancer (TNBC) and determined that PDCD11 acts as an oncogene in TNBC. The cytoplasmic ribosomal protein S6 (RPS6) is a subunit of the 40S subunit (29,30). Shirakawa *et al* (31) demonstrated that RPS6 was present in perinecrotic, perivascular and border niches in GBM tissues and was markedly elevated in high-grade gliomas. To date, >88 clinical trials of immunotherapies for GBM have been initiated and conducted worldwide (32). In addition, several immunotherapies have shown promising efficacy, including

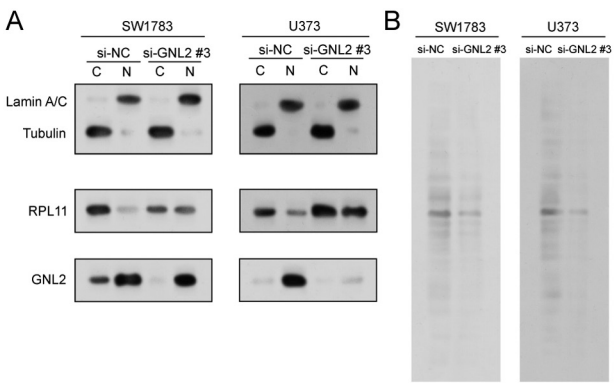

Figure 7. Effects of GNL2 knockdown on ribosomal protein localization and protein synthesis in glioma cells. (A) WB analysis of RPL11 localization in nuclear and cytoplasmic fractions from SW1783 and U373 cells with GNL2 knockdown (siGNL2) or control vectors. Lamin A/C and Tubulin were used as markers for the nuclear and cytoplasmic fractions, respectively. (B) WB analysis demonstrating that GNL2 knockdown inhibits overall protein synthesis in glioma cells (SW1783 and U373). Total protein synthesis was reduced after GNL2 knockdown compared with the si-NC controls. GNL2, G protein nucleolar 2; WB, western blot; NC, negative control; si, small interfering RNA; RPL11, ribosomal protein L11.

dendritic cell (DC) vaccines such as DCVax-L (33) and oncolytic virus G47Δ (34). Furthermore, the swift emergence of molecular subtypes in gliomas carries significant clinical implications and applications. These encompass diagnostic imaging, pathology testing prerequisites, strategic planning for clinical trials and the implementation of targeted therapies for gliomas (35). This consolidated evidence amplifies the potential of these genes as vital prognostic indicators and offers a promising avenue for therapeutic advancements in glioma.

GNL2 enables RNA-binding activity and is predicted to be involved in ribosome biogenesis (17). The GNL2 family encompasses two members, namely GNL3 (nucleoprotein) and GNL3-like (GNL3L) (36). While GNL3L functions as the vertebrate equivalent of the nucleostemin, GNL2 has a unique presence across both vertebrate and invertebrate species (37). The contribution of GNL2 to various cancers has been previously highlighted in the literature. In a compelling study by Nakamura *et al* (17), it was observed that healthy fallopian tube secretory epithelial cells exhibited increased proliferation and colony formation when GNL2 was overexpressed, but xenograft tumor development was inhibited when GNL2 was silenced. Furthermore, within the context of ovarian cancer, GNL2 appears to regulate the formation of the 60S ribosomal subunit (17). Drawing from these existing investigations, GNL2 was deemed a potential biomarker for glioma. The subsequent analyses of the present study revealed that GNL2 levels were markedly elevated in glioma as compared with normal tissues. Furthermore, high expression of GNL2 was associated with diminished survival rates. Collectively, these observations led us to conclude that GNL2 functions as an oncogene within the scope of glioma.

The present study underscores the pivotal role of GNL2 in glioma pathogenesis. Enhanced GNL2 expression was detected in glioma cell lines, particularly SW1783 and U373. Following GNL2 knockdown, a significant reduction in glioma cell proliferation, invasion and migration was observed, highlighting the potential oncogenic and therapeutic importance of GNL2 in glioma. Furthermore, GNL2 seems instrumental in modulating RPL11 subcellular localization and overall protein synthesis. GNL2 silencing resulted in RPL11 nuclear accumulation and a reduced cytoplasmic/nuclear ratio, a novel observation that suggests a potential regulatory mechanism by GNL2 in glioma pathogenesis. Dysregulation of ribosomal proteins such as RPL11, crucial for ribosomal biogenesis, can incite cellular stress and contribute to diseases including cancer (38). In gliomas, manipulation of ribosomal proteins can affect key cellular processes and their overexpression is linked to poor prognosis (39,40). Thus, understanding the role of RPL11 in glioma may provide important molecular insight and potential therapeutic targets. Furthermore, GNL2 silencing inhibited overall protein synthesis, implying GNL2 may govern protein synthesis via RPL11 localization regulation. The current findings suggest a mechanism through which GNL2 influences the oncogenic behavior of glioma, potentially via RPL11, highlighting GNL2's promise as a therapeutic target for glioma. This combined evidence further solidifies the key position of these genes among the prognostic indicators of gliomas and provides a broad perspective for future treatments. The present study revealed the critical role of these genes in tumor development and patient prognosis, laying a foundation for a deeper understanding of glioma biology and disease mechanisms. In-depth study of these genes not only enables more accurate assessment of patient prognosis, but also supports individualized treatment. Understanding gene function and expression patterns can help optimize therapeutic regimens and improve targeting and effectiveness. The findings provide important clues for the development of new therapeutic strategies and are expected to improve the outcome of glioma treatment. The current study lays a foundation for incorporating genetic information into the clinical management of gliomas, facilitating the application of personalized medicine in this field, improving patient survival and quality of life, and pointing the way to future research and clinical practice. Although the present study highlights the critical role of specific genes, possible limitations in sample size and patient heterogeneity need to be recognized, and larger and multicenter studies are needed to address these challenges in the future.

In conclusion, by bioinformatics analysis, 3 promising prognostic biomarkers in glioma were identified in the present study, namely GNL2, PDCD11 and RPS6. Furthermore, GNL2 was investigated as the hub gene in the present study, and it was found to be upregulated in glioma tissues and closely connected with poor prognosis. GNL2 silencing inhibits glioma cell growth and impairs the export of 60S ribosomal subunits and promotes overall protein synthesis in glioma cells. Collectively, GNL2 promotes the protein synthesis of RPL11 to facilitate the development of glioma. All of these findings provide new hints for clinical applications for glioma.

Acknowledgements

Not applicable.

Funding

No funding was received.

Availability of data and materials

The data generated in the present study may be requested from the corresponding author.

Authors' contributions

XY and XL participated in the conception and design of the study, as well as data collection and analysis. XY and XL were involved in drafting the manuscript or revising it critically for intellectual content. XY and XL confirm the authenticity of all the raw data. Both XY and XL read and approved the final version of the manuscript.

Ethics approval and consent to participate

Not applicable.

Patient consent for publication

Not applicable.

Competing interests

The authors declare that they have no competing interests.

References

1. Elia-Pasquet S, Provost D, Jaffré A, Loiseau H, Vital A, Kantor G, Maire JP, Dautheribes M, Darrouzet V, Dartigues JF, *et al*: Incidence of central nervous system tumors in Gironde, France. Neuroepidemiology 23: 110-117, 2004.
2. Persano L, Rampazzo E, Basso G and Viola G: Glioblastoma cancer stem cells: Role of the microenvironment and therapeutic targeting. Biochem Pharmacol 85: 612-622, 2013.
3. Reddy AT and Wellons JC III: Pediatric high-grade gliomas. Cancer J 9: 107-112, 2003.
4. Perkins SM, Rubin JB, Leonard JR, Smyth MD, El Naqa I, Michalski JM, Simpson JR, Limbrick DL, Park TS and Mansur DB: Glioblastoma in children: A single-institution experience. Int J Radiat Oncol Biol Phys 80: 1117-1121, 2011.
5. Bălașa A, Șerban G, Chinezu R, Hurghiș C, Tămaș F and Manu D: The involvement of exosomes in glioblastoma development, diagnosis, prognosis, and treatment. Brain Sci 10: 553, 2020.
6. Seymour T, Nowak A and Kakulas F: Targeting aggressive cancer stem cells in glioblastoma. Front Oncol 5: 159, 2015.
7. Anji A and Kumari M: Guardian of genetic messenger-RNA-binding proteins. Biomolecules 6: 4, 2016.
8. Hentze MW, Castello A, Schwarzl T and Preiss T: A brave new world of RNA-binding proteins. Nat Rev Mol Cell Biol 19: 327-341, 2018.
9. Muleya V and Marondedze C: Functional roles of RNA-Binding Proteins in plant signaling. Life 10: 288, 2020.
10. Idler RK and Yan W: Control of messenger RNA fate by RNA-binding proteins: An emphasis on mammalian spermatogenesis. J Androl 33: 309-337, 2012.
11. Li X, Zhang F, Ma J, Ruan X, Liu X, Zheng J, Liu Y, Cao S, Shen S, Shao L, *et al*: NCBP3/SNHG6 inhibits GBX2 transcription in a histone modification manner to facilitate the malignant biological behaviour of glioma cells. RNA Biol 18: 47-63, 2021.
12. Gerstberger S, Hafner M and Tuschl T: A census of human RNA-binding proteins. Nat Rev Genet 15: 829-845, 2014.
13. Schmittgen TD, Livak KJ: Analyzing real-time PCR data by the comparative C(T) method. Nat Protoc 3: 1101-1108, 2008.
14. Tailler M, Lindqvist LM, Gibson L and Adams JM: By reducing global mRNA translation in several ways, 2-deoxyglucose lowers MCL-1 protein and sensitizes hemopoietic tumor cells to BH3 mimetic ABT737. Cell Death Differ 26: 1766-1781, 2019.
15. Okuwaki M, Saito S, Hirawake-Mogi H and Nagata K: The interaction between nucleophosmin/NPM1 and the large ribosomal subunit precursors contribute to maintaining the nucleolar structure. Biochim Biophys Acta Mol Cell Res 1868: 118879, 2021.
16. Yelland JN, Bravo JPK, Black JJ, Taylor DW and Johnson AW: A single 2'-O-methylation of ribosomal RNA gates assembly of a functional ribosome. Nat Struct Mol Biol 30: 91-98, 2023.
17. Nakamura K, Reid BM, Chen A, Chen Z, Goode EL, Permuth JB, Teer JK, Tyrer J, Yu X, Kanetsky PA, *et al*: Functional analysis of the 1p34.3 risk locus implicates GNL2 in high-grade serous ovarian cancer. Am J Hum Genet 109: 116-135, 2022.
18. Ostrom QT, Bauchet L, Davis FG, Deltour I, Fisher JL, Langer CE, Pekmezci M, Schwartzbaum JA, Turner MC, Walsh KM, *et al*: The epidemiology of glioma in adults: a 'state of the science' review. Neuro Oncol 16: 896-913, 2014.
19. Xiao H, Ding N, Liao H, Yao Z, Cheng X, Zhang J and Zhao M: Prediction of relapse and prognosis by expression levels of long noncoding RNA PEG10 in glioma patients. Medicine (Baltimore) 98: e17583, 2019.
20. Delgado-López P and Corrales-García E: Survival in glioblastoma: A review on the impact of treatment modalities. Clin Transl Oncol 18: 1062-1071, 2016.
21. Van Meir EG, Hadjipanayis CG, Norden AD, Shu HK, Wen PY and Olson JJ: Exciting new advances in neuro-oncology: The avenue to a cure for malignant glioma. CA Cancer J Clin 60: 166-193, 2010.
22. Wohlfart S, Khalansky AS, Gelperina S, Maksimenko O, Bernreuther C, Glatzel M and Kreuter J: Efficient chemotherapy of rat glioblastoma using doxorubicin-loaded PLGA nanoparticles with different stabilizers. PLoS One 6: e19121, 2011.
23. Chow AKM, Yau SWL and Ng L: Novel molecular targets in hepatocellular carcinoma. World J Clin Oncol 11: 589-605, 2020.
24. Chaillou T, Kirby TJ and McCarthy JJ: Ribosome biogenesis: Emerging evidence for a central role in the regulation of skeletal muscle mass. J Cell Physiol 229: 1584-1594, 2014.
25. Henras AK, Plisson-Chastang C, O'Donohue MF, Chakraborty A and Gleizes PE: An overview of pre-ribosomal RNA processing in eukaryotes. Wiley Interdiscip Rev RNA 6: 225-242, 2015.
26. Yoshida Y, Wang H, Hiwasa T, Machida T, Kobayashi E, Mine S, Tomiyoshi G, Nakamura R, Shinmen N, Kuroda H, *et al*: Elevation of autoantibody level against PDCD11 in patients with transient ischemic attack. Oncotarget 9: 8836-8848, 2017.
27. Eid W, Hess D, König C, Gentili C and Ferrari S: The human exonuclease-1 interactome and phosphorylation sites. Biochem Biophys Res Commun 514: 567-573, 2019.
28. Xing Z, Wang R, Wang X, Liu J, Zhang M, Feng K and Wang X: CircRNA circ-PDCD11 promotes triple-negative breast cancer progression via enhancing aerobic glycolysis. Cell Death Discov 7: 218, 2021.
29. Williams AJ, Werner-Fraczek J, Chang IF and Bailey-Serres J: Regulated phosphorylation of 40S ribosomal protein S6 in root tips of maize. Plant Physiol 132: 2086-2097, 2003.
30. Cuperjani F, Gashi L, Kurshumliu F, Dreshaj S and Selimi F: Relationship between ribosomal protein S6-pS240 expression and other prognostic factors in non-special type invasive breast cancer. Breast Care (Basel) 14: 171-175, 2019.
31. Shirakawa Y, Ohta K, Miyake S, Kanemaru A, Kuwano A, Yonemaru K, Uchino S, Yamaoka M, Ito Y, Ito N, *et al*: Glioma cells acquire stem-like characters by extrinsic ribosome stimuli. Cells 10: 2970, 2021.
32. Mahmoud AB, Ajina R, Aref S, Darwish M, Alsayb M, Taher M, AlSharif SA, Hashem AM and Alkayyal AA: Advances in immunotherapy for glioblastoma multiforme. Front Immunol 13: 944452, 2022.
33. Liau LM, Ashkan K, Brem S, Campian JL, Trusheim JE, Iwamoto FM, Tran DD, Ansstas G, Cobbs CS, Heth JA, *et al*: Association of autologous tumor lysate-loaded dendritic cell vaccination with extension of survival among patients with newly diagnosed and recurrent glioblastoma: A phase 3 prospective externally controlled cohort trial. JAMA Oncol 9: 112-121, 2023.
34. Todo T, Ito H, Ino Y, Ohtsu H, Ota Y, Shibahara J and Tanaka M: Intratumoral oncolytic herpes virus G47 for residual or recurrent glioblastoma: A phase 2 trial. Nat Med 28: 1630-1639, 2022.
35. Chen R, Smith-Cohn M, Cohen AL and Colman H: Glioma subclassifications and their clinical significance. Neurotherapeutics 14: 284-297, 2017.
36. Quiroga-Artigas G, de Jong D and Schnitzler CE: GNL3 is an evolutionarily-conserved stem cell gene influencing cell proliferation, animal growth, and regeneration in the hydrozoan Hydractinia. Open Biol 12: 220120, 2022.
37. Dong Y, Cai Q, Fu L, Liu H, Ma M and Wu X: Study of the G protein nucleolar 2 value in liver hepatocellular carcinoma treatment and prognosis. Biomed Res Int 2021: 4873678, 2021.
38. Kang J, Brajanovski N, Chan KT, Xuan J, Pearson RB and Sanij E: Ribosomal proteins and human diseases: Molecular mechanisms and targeted therapy. Signal Transduct Target Ther 6: 323, 2021.
39. Guo P, Wang Y, Dai C, Tao C, Wu F, Xie X, Yu H, Zhu Q, Li J, Ye L, *et al*: Ribosomal protein S15a promotes tumor angiogenesis via enhancing Wnt/β-catenin-induced FGF18 expression in hepatocellular carcinoma. Oncogene 37: 1220-1236, 2018.
40. Elhamamsy AR, Metge BJ, Alsheikh HA, Shevde LA and Samant RS: Ribosome biogenesis: A central player in cancer metastasis and therapeutic resistance. Cancer Res 82: 2344-2353, 2022.